Molecular Imaging of Infectious Diseases

34

Anna-Maria Rolle and Stefan Wiehr

Contents

Despite the success of therapeutics fighting against especially bacteria and fungi, infectious diseases still remain one of the main causes of death worldwide (WHO 2014). Besides effective medication, the early and reliable differential diagnosis of infectious diseases is of utmost importance; here noninvasive imaging can have a huge impact. The host defense against pathogens is dependent on an intact innate and adaptive immune response and effective communication between the immune cells. Dysfunction of one or more of these immune compartments leads to an open gateway for pathogens into the body of humans and animals. Infection is often accompanied with inflammation but both processes differ from each other. Inflammation is basically a nonspecific immune response which can have many reasons but does not necessarily require a microorganism in the inflamed site (Petruzzi et al. 2009). Very well-adapted pathogens have evolved strategies to act immunomodulatory to evade the immune response of the host and to finally enable their survival and transmission (Coombes and Robey 2010).

Traditional, laboratory-based diagnostic modalities such as blood cultures, PCR, antigen tests, and microscopy often result in long turnaround times, making it more difficult when dealing with contaminants thereby compelling clinicians to treat patients empirically with broad-spectrum medication until diagnostic results are available (Bates et al. 1997; Nakamura et al. 2006; Weinstein et al. 2014). Molecular

A.-M. Rolle (✉) • S. Wiehr
Werner Siemens Imaging Center, Department of Preclinical Imaging and Radiopharmacy, Eberhard Karls University Tübingen, Tübingen, Germany
e-mail: Anna-Maria.Rolle@med.uni-tuebingen.de

F. Kiessling et al. (eds.), *Small Animal Imaging*, DOI 10.1007/978-3-319-42202-2_34

imaging has the potential to early and accurately detect infections and monitor treatment efficacies, thereby limiting incorrect or unnecessary treatment and the intrinsic burden of cost, drug resistance, and damage to the patient's health (Stevens et al. 2014; Weinstein et al. 2014). There are several challenging aspects of imaging infectious diseases, not at least the clear and reliable differentiation between fungal, parasitic, bacterial, and viral infection, which is needed for the best treatment option. Furthermore, infection is typically linked to inflammation which makes it mandatory to employ pathogen-specific imaging probes to definitively and rapidly diagnose the causative agent of the infectious disease.

Existing clinically used tracers for PET or SPECT imaging are not able to distinguish between malignancies and sterile or pathogen-induced inflammations or the infectious entities (Bunschoten et al. 2013; Dorward et al. 2012; Signore et al. 2010; Smith et al. 2013). Furthermore, at the late stages of the infection, it is even more challenging to correctly diagnose the cause of illness as the disease can manifest with nonpathogen-induced symptoms resembling malignancies (Glaudemans and Signore 2010). In general, the main problem of identifying the cause of the infectious disease – the pathogen – with the help of imaging methods is to use specific markers for the respective pathogen, which are rarely or not at all available. It has to be noted that most of the used radiopharmaceuticals detect nonspecific inflammation sites but do not accumulate in the pathogen. Because of the lack of a specific marker in nuclear medicine techniques, in most cases invasive puncture or biopsy of tissue or fluids is required to confirm the presence of the infectious pathogens with molecular biology techniques. Those laboratory tests are time-consuming and lack sensitivity and specificity delaying a clear diagnosis and therefore optimal treatment stratification for patients.

Various radiopharmaceuticals were developed and evaluated in both preclinical and clinical studies as potential diagnostic agents to identify the sites of infection (Goldsmith and Vallabhajosula 2009). Arguably, the main limitation to imaging of infectious microorganisms is the availability of pathogen-specific markers. Most of the currently available radiopharmaceuticals detect nonspecific inflammation sites but do not accumulate in microorganisms. Radionuclide imaging with gallium 67 citrate, the most widely used agent for detecting inflammation and infection, is not specific and has the additional disadvantages of long imaging time, low resolution, and high patient radiation dose. The uptake of the radiometal in the liver, the kidneys, and other organs has limited its use for diagnosis of various diseases (Dumarey et al. 2006; Parisi 2011). In vitro radiolabeling of leukocytes with ^{111}In or ^{99m}Tc is considered the gold standard for infection imaging. The radiolabeled leukocytes injected in patients migrate to the sites of infection/inflammation allowing imaging of infectious foci (Parisi 2011). The labeling of leukocytes in vitro requires an expensive and time-consuming procedure with the associated risks of contamination (Petruzzi et al. 2009).

Fluorine-18 fluorodeoxyglucose (^{18}F-FDG), the major clinical PET tracer used for the detection of malignancies, has been used for imaging of infectious diseases or their inflammatory processes (Jamar et al. 2013). However, as a general indicator of metabolic activity of cells, it does not allow the specific identification of pathogens at sites of inflammation (del Rosal et al. 2013).

The PET tracer ^{18}F-FLT, as a surrogate marker for cell proliferation, which is used in the clinics, is primarily used for the detection of cancer cells and has received little attention as a possible tracer for inflammation and infectious disease diagnosis (van Waarde et al. 2004). In the salvage pathway, ^{18}F-FLT is transported across the cell membrane by nucleoside carrier proteins and phosphorylated by the S-phase-specific thymidine kinase 1 (TK-1), which leads to trapping of the tracer in the cytosol as monophosphate without DNA incorporation and subsequent availability as a substrate for cytoplasmic TK-1 (Bading and Shields 2008; Shields et al. 1998). However, ^{18}F-FLT PET does not always correlate with proliferation and, in the preclinical animal setting, is dependent on anesthesia and available serum thymidine, which can compete with ^{18}F-FLT for nucleoside carrier proteins (Cobben et al. 2003;

Fuchs et al. 2013a, b; McKinley et al. 2013, 2014; Nottebrock and Then 1977). So far the proliferation marker ^{18}F-FLT is not suitable to image bacterial, fungal, or parasitic infections.

An increasing number of innovative PET radiopharmaceuticals, employing monoclonal antibodies or their fragments, peptides, and small molecules, have been developed and evaluated for infectious disease imaging (Glaudemans et al. 2012), but compared to cancer research, tracer development for the specific detection of fungi and parasites is in its infancy. Nevertheless, whole-body PET imaging combined with functional magnetic resonance imaging (fMRI) including perfusion imaging, diffusion-weighted imaging (DWI), and magnetic resonance spectroscopy (MRS) has begun to provide valuable insights into host-pathogen interactions (Signore and Glaudemans 2011), permitting real-time in vivo monitoring of pathogen distributions within the infected host, and will lead to better understanding of the biology of the pathogen causing a disease.

Many efforts have already been made to gain further insights in the parasite's or micropathogen's life inside its host (Coombes and Robey 2010). Bioluminescence imaging, two-photon laser scanning microscopy, and intravital imaging techniques are attractive imaging methods because of comparable low costs. Optical imaging can be divided into fluorescence- and bioluminescence-based methods. Intravital imaging can visualize cell-cell or cell-protein interactions, which is not possible with PET or MRI. The drawback of intravital imaging is its invasiveness and the small field of view. The fundamental limitation and disadvantage of optical imaging are the low tissue penetration of light and the lack of absolute quantification of the imaging results.

Various in vitro and in vivo labeling methods are established for labeling cells and are depicted in Fig. 34.1 (Ahrens and Bulte 2013; Kircher et al. 2011). Two major principles for imaging and tracking of cells, direct and indirect labeling, are described by Kirchner et al. (2011). Direct labeling of cells or pathogens is the simplest method, but the label can be diluted by proliferation of the cells and organisms or released during the time. For direct labeling methods in PET, long-lived isotopes are used, such as Cu-64 ($T_{1/2}$ = 12.7) which is generated as ^{64}Cu-PTSM (Griessinger et al. 2014). Genetically engineered cells or organisms are used for indirect labeling methods where reporter genes are introduced into the cell DNA and translated into enzymes, receptors, fluorescence proteins, or bioluminescence luciferase (Coombes et al. 2013; Hasenbach et al. 2012; Kircher et al. 2011). The advantage of stable transfected microorganisms is the possibility of monitoring labeled pathogens or cells over their entire lifetime either with optical imaging methods or with PET/MRI. For the latter, a specific tracer is needed which accumulates within the transfected cell and can be repeatedly injected into the animal after decay of the used radioisotope. The herpes simplex virus thymidine kinase type 1 (HSV-1 TK) is an often used reporter gene for PET imaging because of its restriction to viruses and absence in eukaryotic cells (Hasenbach et al. 2012). PET tracers are, for example, a fluorine-18-labeled acycloguanosine derivative substrate (9-(4-^{18}F-fluoro-3-hydroxymethylbutyl)guanine, ^{18}F-FHBG) for HSV-1 TK and 2′-deoxy-2′-^{18}F-fluoro-5-ethyl-1-β-d-arabinofuranosyluracil (^{18}F-FEAU) where the thymidine kinase phosphorylates the radioactive nucleoside analog substrate, thereby accumulating the tracer into the HSV-1 TK-expressing cell (Kircher et al. 2011). The disadvantage of these tracers is the high unspecific uptake in various organs. Without having the anatomical information of MRI, it is virtually impossible to identify the faint uptake of the tracer in spots where the HSV-1 TK-expressing cells accumulate (Hasenbach et al. 2012).

The rare and chronic zoonotic parasitic disease alveolar echinococcosis (AE) is caused by the larval form (metacestode) of the cestode *Echinococcus multilocularis*, known as the fox tapeworm (Eckert and Deplazes 2004; Tappe et al. 2010). This cancer-mimicking disease is detected in the northern hemisphere including Middle and Eastern Europe, North America, Northern Asia, China, and Japan (Eckert and Deplazes 2004; Knapp et al. 2009). In the advanced stage of the infection, the parasite

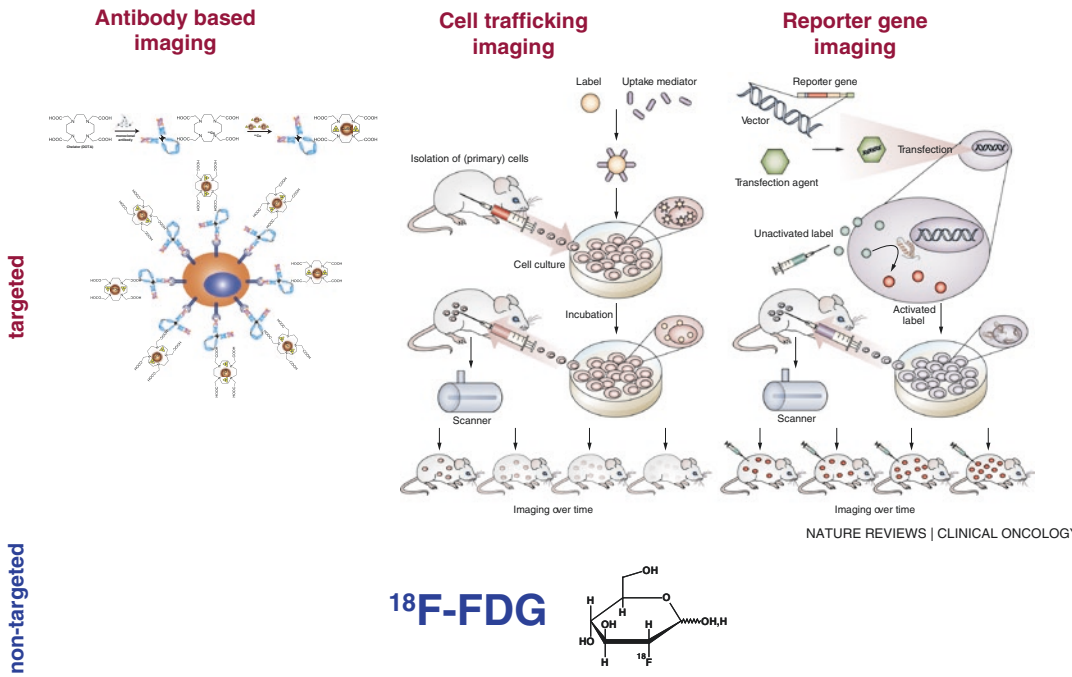

Fig. 34.1 Principles of direct and indirect labeling methods for targeted imaging. For direct labeling of cells, exogenous markers are coupled to a radiolabeled antibody, a transfection agent, or a positively charged peptide and then incubated with cells. Primary cells, such as lymphocytes, are first harvested from a donor, conjugated with a suitable label, and subsequently cells are introduced into the recipient for repeated scanning. Since the label diffuses out of cells and is diluted during cell division, imaging is only feasible over a limited period of time. Indirect cell labeling with reporter genes requires genetic modification of the cells. Cells are transfected with a vector that contains a promoter, which regulates expression of the reporter gene. Such genes can encode receptors, fluorescent proteins, or enzymes, which activate the imaging probe or mediate its accumulation within the cell. Transfected cells are expanded in cell culture before injection. With the exception of fluorescent reporter proteins, each imaging session requires injection of the label, which marks only the transfected cells. In stably transfected cells, the vector is passed on to daughter cells, and cell expansion can be imaged (Adapted from Kircher et al. (2011))

disseminates via the blood or lymphatic vessels to other adjacent organs including the lungs but also to the brain (Tuzun et al. 2002). The proliferation of the metacestode is accompanied by invading immune cells around the multi-chambered cystic structures causing inflammation and necrosis in the periparasitic granuloma (Mejri et al. 2010; Vuitton and Gottstein 2010). The clinical PET tracer ^{18}F-FDG has previously been reported to be useful for the diagnostic and therapy follow-up of AE patients (Reuter et al. 1999; 2008). Nevertheless, small lesions are consistently detected with less reliability, especially in organs with high background activity such as the liver, which possibly leads to false-negative findings. In Fig. 34.2 an *Echinococcus multilocularis*-infected gerbil (*Meriones unguiculatus*) was imaged with PET/MRI using either ^{18}F-FDG or ^{18}F-FLT (Rolle et al. 2015). The disadvantage of the PET tracers ^{18}F-FDG and ^{18}F-FLT is the already mentioned unspecific uptake of glucose and the proliferation marker in the inflamed tissue surrounding the parasite tissue but not by the parasite itself (Rolle et al. 2015).

^{11}C-Choline, another promising tracer that detects membrane synthesis, is first phosphorylated within the cell and then trapped into lecithin of the cell membrane as phosphatidylcholine (Hara 2002). Concentrations of various metabolites in cerebral alveolar echinococcosis lesions were investigated by proton magnetic resonance spectroscopy (^{1}PMRS), and their changes

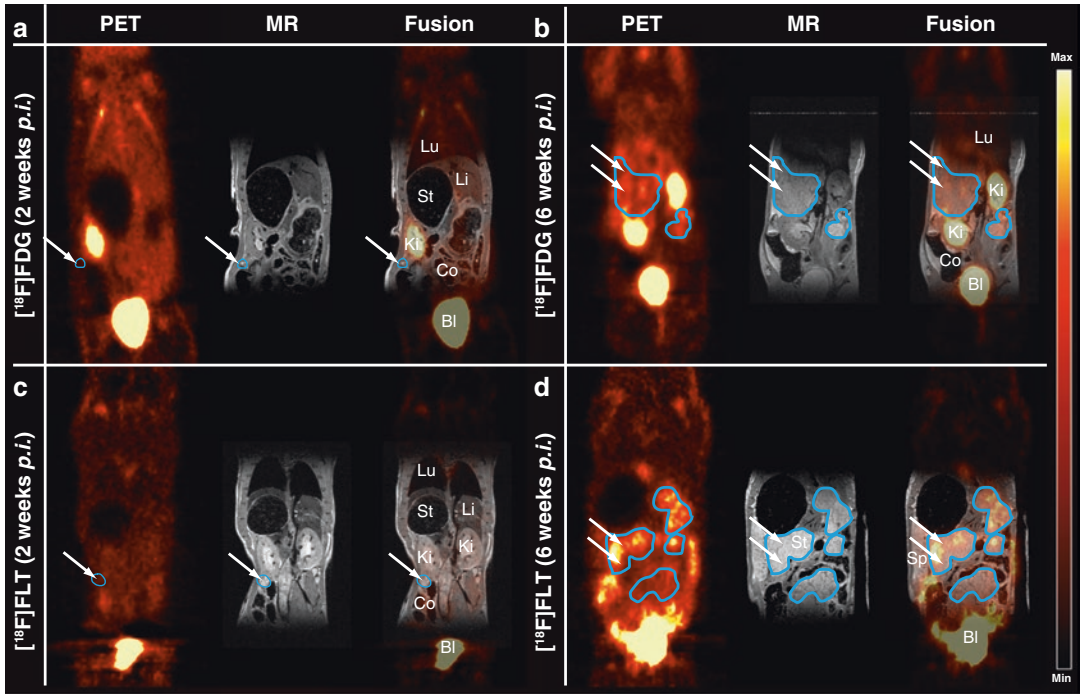

Fig. 34.2 Coronal ^{18}F-FDG or ^{18}F-FLT PET, MR, and fused images from early (*2 weeks p.i.*, **a**, **c**)- and late (*6 weeks p.i.*, **b**, **d**)-stage *E. multilocularis* metacestode-infected gerbils. *Arrows* and *blue lines* indicate the positions of the metacestode tissue (*Bl* bladder, *Co* colon, *Ki* kidney, *Li* liver, *Lu* lung, *Sp* spleen, *St* stomach) (Rolle et al. 2015)

depending on the region of the parasitic mass were recorded. Choline was found to have the highest concentration in the substantial area of the lesions (Wang et al. 2012). A high uptake of ^{11}C-choline in *E. multilocularis* vesicles in cell culture binding assays was observed (Rolle et al. 2015) because choline is quickly integrated as a precursor for the biosynthesis of phospholipids, which are important components of all membranes (Hara 2002). However, the in vivo studies with ^{11}C-choline showed no accumulation in the parasitic lesions in late-stage AE-infected animals (Fig. 34.3a) (Rolle et al. 2015).

Hypoxic regions can be identified using the ^{18}F-fluoro-azomycinarabinofuranoside (^{18}F-FAZA), a 2-nitroimidazole PET tracer. ^{18}F-FAZA is diffusible through cell membranes and undergoes reversible reduction. Therefore, with decreasing intracellular concentration of oxygen, the tracer accumulates within the hypoxic tissue (Marik and Junutula 2011). In preclinical settings and in patients, ^{18}F-FAZA is a widely studied PET tracer for the identification of hypoxic areas within tumors (Beck et al. 2007; Maier et al. 2011; Sorger et al. 2003). Although there have been reports of hypoxia playing an important role in infectious diseases, ^{18}F-FAZA has not been used to date for the detection of infected areas. In vitro binding assays displayed a slightly elevated uptake of ^{18}F-FAZA in *E. multilocularis* vesicles; however, this tracer also revealed to be not applicable for the detection of *E. multilocularis* parasitic lesions at least in the animal model (Fig. 34.3b) (Rolle et al. 2015).

All tested small molecules and clinically used tracers showed elevated uptake pattern in cell culture experiments, which could not be confirmed by the in vivo experiments. A different approach is the use of radiolabeled antibodies specific to the pathogen for PET/MRI. This method is already realized in the preclinical and clinical field of antibody-guided immunoPET (Wiehr et al. 2014) and can be easily transferred to the emerging field of infectious disease

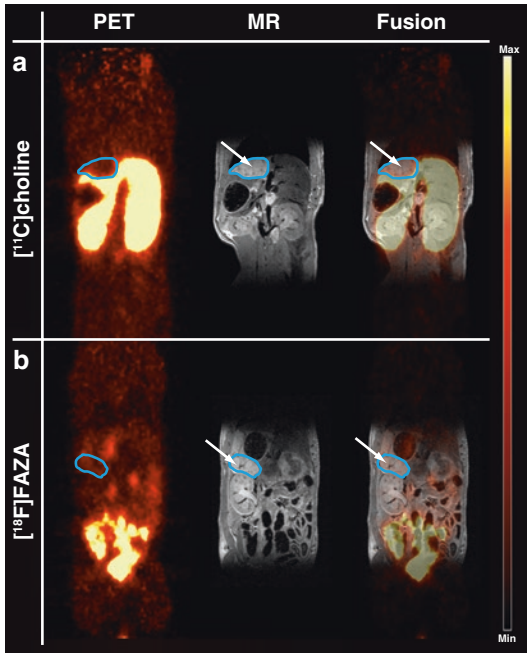

Fig. 34.3 Coronal ^{18}F-FAZA (**a**) and ^{11}C-choline (**b**) PET, MR, and fused images from late (6 weeks *p.i.*)-stage *E. multilocularis* metacestode-infected gerbils. *Arrows* and *blue lines* indicate the positions of the metacestode tissue. Only background uptake of these tracers is observed in the parasite tissue (Rolle et al. 2015)

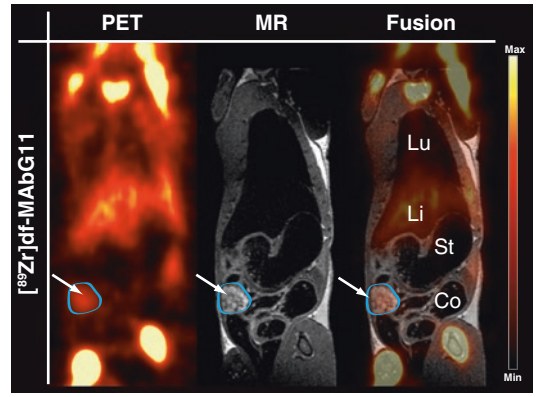

Fig. 34.4 Coronal PET, MR and fused images from early stage *E. multilocularis* metacestode infected gerbils imaged with ^{89}Zr-desferal labeled monoclonal antibody MabG11. *Arrows* and blue lines indicate the localization of the metacestode tissue (*Co* colon, *Ki* kidney, *Li* liver, *Lu* lung, *St* stomach)

imaging. In contrast to the small-molecule (unspecific) PET tracers, a radiolabeled *E. multilocularis*-specific monoclonal antibody binds to the vesicle membrane of the metacestode and clearly depicts the presence of the parasite. In combination with the superior soft tissue contrast of the MRI and the specific marker for PET, PET/MRI can serve as an emerging tool to explicitly identify and diagnose the alveolar echinococcosis disease and exclude it from other cystic liver diseases (Fig. 34.4).

Newly developed disease-specific tracers might be used alongside emerging molecular imaging technologies such as combined PET/MRI to obtain highly accurate spatially and temporally aligned multiparametric molecular, functional, and morphological data of disease progression. Humans with impaired immunity, e.g., those with hematological malignancies or bone marrow transplant recipients, are at a substantially elevated risk of severe, invasive *Aspergillus fumigatus* infection known as invasive pulmonary aspergillosis (IPA) (Brown et al. 2012). Diagnosis of IPA is a major challenge as clinical manifestations of the disease (febrile episodes unresponsive to antibiotics, pulmonary infiltrates, and radiological abnormalities) are nonspecific and methods for the detection of circulating biomarkers such as β-D-glucan or galactomannan (GM) in the bloodstream lack specificity or sensitivity (Freifeld et al. 2011). A convenient, fast, and specific diagnosis of IPA is currently not available, forcing clinicians to implement empiric treatments with costly and toxic antifungal drugs once standard antibiotics have failed to reduce fever in patients with fever of unknown origin (FUO). Consequently, there is the potential to increase the survival rates of aspergillosis patients, if a definitive diagnosis of IPA could be obtained early and its response to treatment monitored and adjusted accordingly.

While it has been reported that ^{18}F-FDG might serve as a useful imaging tool for initial diagnosis and therapy monitoring of IA (Hot et al. 2011), our investigations have shown that increased ^{18}F-FDG uptake in *A. fumigatus*-infected lungs is indistinguishable from the uptake seen during inflammatory reactions due to sterile triggers or other pathogens (Rolle et al. 2016). Attempts have been made to visualize IPA in *A.*

fumigatus-infected animals with microPET/CT using ^{68}Ga radiolabeled siderophores (Haas et al. 2015; Petrik et al. 2010). These small high-affinity chelating compounds are produced by fungi and bacteria to scavenge iron from the host and by gram-negative bacterial pathogens as virulence factors (Holden and Bachman 2015). While rapid uptake of ^{68}Ga by the *A. fumigatus* siderophore TAFC has been shown to occur under conditions of iron depletion, TAFC-mediated ^{68}Ga uptake has also been demonstrated in *Fusarium solani* and *Rhizopus oryzae*, invasive fungal pathogens that cause fusariosis and mucormycosis in immunocompromised patients (Thornton and Wills 2015).

Recently, *A. fumigatus* detection based on single-photon emission computerized tomography (SPECT) with ^{99m}Tc-labeled morpholino oligonucleotides (MORFs) specific for fungal 28S rRNA has been investigated (Wang et al. 2013). While *A. fumigatus* lung infections are clearly discerned using this technique, further investigations in other infectious models are needed to confirm the specificity of this probe.

ImmunoPET has recently been used for tracking simian immunodeficiency virus (SIV) infection in macaques (Santangelo et al. 2015), and another example of the rapid and specific detection of the lethal fungal infection IPA with immunoPET is depicted in Fig. 34.5 (Rolle et al. 2016). *A. fumigatus*-infected, neutropenic mice were imaged with an anti-*Aspergillus* PET marker. The ^{64}Cu-DOTA-labeled anti-*Aspergillus* mAb JF5 was intravenously (*i.v.*) injected, and subsequent PET images were acquired, which show the localization of the tracer in the lungs of infected mice 48 h after the initial pulmonary infection. Due to the long in vivo half-life of the copper-64-radiolabeled mAb specific to *Aspergillus*, the immunoPET approach is able to detect fungal colonization at all stages of mycelial growth and is possibly useful for treatment monitoring. The hyphal-specific nature of our immunoPET tracer may therefore prove useful in monitoring infection in response to antifungal treatment (Rolle et al. 2016).

Several PET tracers for bacterial infections have been developed and tested in preclinical studies using antibiotics, peptides, antibodies, and radiolabeled white blood cells, but have so far had limited clinical impact (Bunschoten et al. 2013; Ning et al. 2014). Radiolabeled antibiotics are active at low concentrations and are therefore not the best candidates for molecular imaging. Clinical studies, for example, with ^{99m}Tc-ciproflaxin, have also shown limited specificity (Langer et al. 2005; Sarda et al. 2003; Vinjamuri et al. 1996; Weinstein et al. 2014).

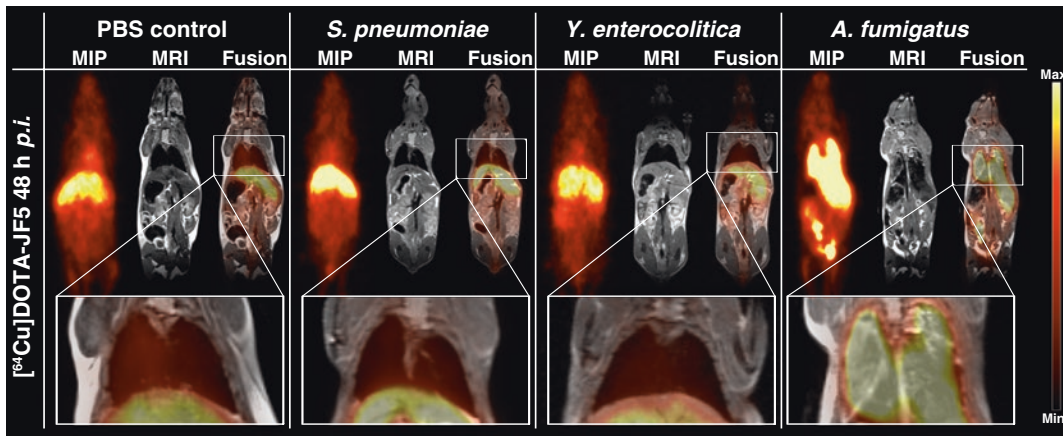

Fig. 34.5 Coronal maximum intensity projection (*MIP*), magnetic resonance imaging (*MRI*), and fused positron emission tomography (PET)/MRI images of PBS-treated and *Streptococcus pneumoniae*-, *Yersinia enterocolitica*-, and *Aspergillus fumigatus*-infected mice injected with ^{64}Cu-DOTA-JF5 (48 h after infection). Images demonstrate highly specific tracer accumulation in *A. fumigatus*-infected lung tissue compared to bacterial-infected or sham-treated animals. Lungs of the respective animals are detailed in the *lower panel* (Rolle et al. 2016)

Recently, bacteria-specific PET tracers have been developed with promising preclinical results. Sugar transporters for sorbitol and maltose or an alternative sugar transporter, the bacterial universal hexose phosphate transporter (UHPT), has been investigated as targets for bacteria-specific imaging using 2-^{18}F-fluorodeoxysorbitol (^{18}F-FDS) (Weinstein et al. 2014), 6-^{18}F-fluoromaltose (MH^{18}F) (Ning et al. 2014), and the analog of glucose ^{18}F-FDG-6-P (Mills et al. 2015). Using these tracers it is possible to distinguish between gram-negative (e.g., *Enterobacteriaceae*) and gram-positive (e.g., *Staphylococcus aureus*) bacteria.

The gram-negative bacterium *Yersinia enterocolitica* belongs to the family of *Enterobacteriaceae* and is an important cause of gastrointestinal infections. Infections are caused by ingestion of contaminated food or drinking water and can cause severe diarrhea and enterocolitis (Schindler et al. 2012). In immunocompromised patients, systemic infection can lead to focal abscesses in the spleen and liver (Bottone 1997). The virulence of *Y. enterocolitica* is associated with *Yersinia* adhesin A (YadA), a trimeric autotransporter expressed on the surface that mediates cell adhesion and is an ideal biomarker candidate for the specific imaging of yersiniosis (Di Genaro et al. 2003). A radiolabeled anti-YadA antibody is able to specifically detect the pathogen in vivo. Furthermore, the antibody uptake occurred in an infection dose-dependent manner in the spleen of low-dose infected animals. In contrast, elevated uptake of the standard PET tracer ^{18}F-FDG was only observed in the spleen of high-dose *Y. enterocolitica*-infected mice, although blood glucose levels were raised in both low- and high-dose infected animals (Fig. 34.6). The most likely explanation for this is the induction of inflammation and ^{18}F-FDG uptake by activated immune cells (del Rosal et al. 2013; Rolle et al. 2015) rather than by the bacteria themselves as there was no correlation with the bacterial load. Consequently, these results argue against the use of ^{18}F-FDG for imaging bacterial infections. This is in agreement with the findings of other groups showing that ^{18}F-FDG is highly unspecific in PET oncology, resulting in high rates of false positives (Chacko et al. 2003; Culverwell et al. 2011; Lukawska et al. 2014; Rosenbaum et al. 2006; Stumpe et al. 2000). Furthermore, it is unable to detect early-stage bacterial infections and in some instances shows increased signal intensities after effective antibiotic treatment (Davis et al. 2009; Jain et al. 2005). Nevertheless, it is currently the principal tracer for imaging infectious diseases in humans (Corstens and van der Meer 1999; Glaudemans and Signore 2010; van Oosten et al. 2013).

Many other diseases might benefit from a rapid specific diagnostic tool with PET/MRI replacing

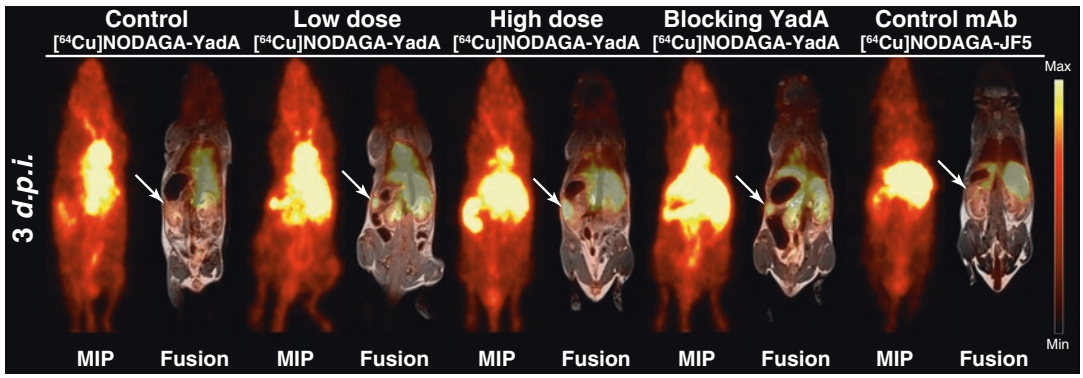

Fig. 34.6 Coronal [^{64}Cu]NODAGA-YadA PET and fused PET and MR images (fusion) from PBS-treated control, low- and high-dose infected mice 3 days *p.i.* Administration of the non-radiolabeled antibody specific to YadA 3 h prior to the injection of the radiolabeled antibody (blocking YadA) or administration of an *A. fumigatus*-specific tracer (control mAb) into high-dose infected mice served as controls. *Arrows* indicate the positions of the spleens, where infectious foci are located, of the mice

cost-intensive, time-consuming, and possible wrong therapeutic decisions. Not at least the non-invasive disease-specific diagnosis with PET/MRI will spare patients from extremely unpleasant and possibly dangerous invasive diagnostic procedures. Using nuclear medicine isotopes with long half-lives for radiolabeling, the biomarker specific for the respective disease, consecutive imaging, and monitoring the success of the therapeutic approach can be achieved with a single application of the diagnostic marker reducing the radiation dose drastically compared to the same number of applied PET/CT measurements. The advantages of simultaneous PET/MRI compared to PET/CT systems are reviewed by Glaudemans et al., pointing out the identical position of the patient in both modalities during acquisition, the functional information of the MRI complementing the molecular information of the PET, the outstanding localization of the PET signal in the soft tissue, and not at least the absence of radiation burden from the MRI system (Glaudemans et al. 2012). The chance to image infectious diseases at an early stage of the disease and at a molecular and cellular level might improve diagnostic potentials and could provide new insights in drug development and so far enigmatic parasite-host interactions. The precise discrimination between infectious disease and inflammation might also solve decisions of the correct therapy.

References

Ahrens ET, Bulte JW. Tracking immune cells in vivo using magnetic resonance imaging. Nat Rev Immunol. 2013;13:755–63.

Bading JR, Shields AF. Imaging of cell proliferation: status and prospects. J Nucl Med. 2008;49 Suppl 2:64S–80.

Bates DW, Sands K, Miller E, Lanken PN, Hibberd PL, Graman PS, Schwartz JS, Kahn K, Snydman DR, Parsonnet J, et al. Predicting bacteremia in patients with sepsis syndrome. Academic Medical Center Consortium Sepsis Project Working Group. J Infect Dis. 1997;176:1538–51.

Beck R, Roper B, Carlsen JM, Huisman MC, Lebschi JA, Andratschke N, Picchio M, Souvatzoglou M, Machulla HJ, Piert M. Pretreatment 18F-FAZA PET predicts success of hypoxia-directed radiochemotherapy using tirapazamine. J Nucl Med. 2007;48:973–80.

Bottone EJ. Yersinia enterocolitica: the charisma continues. Clin Microbiol Rev. 1997;10:257–76.

Brown GD, Denning DW, Gow NA, Levitz SM, Netea MG, White TC. Hidden killers: human fungal infections. Sci Transl Med. 2012;4:165rv113.

Bunschoten A, Welling MM, Termaat MF, Sathekge M, van Leeuwen FW. Development and prospects of dedicated tracers for the molecular imaging of bacterial infections. Bioconjug Chem. 2013;24:1971–89.

Chacko TK, Zhuang H, Nakhoda KZ, Moussavian B, Alavi A. Applications of fluorodeoxyglucose positron emission tomography in the diagnosis of infection. Nucl Med Commun. 2003;24:615–24.

Cobben DC, Elsinga PH, van Waarde A, Jager PL. Correspondence re: H. Barthel et al., 3′-deoxy-3′-[(18)F]fluorothymidine as a new marker for monitoring tumor response to antiproliferative therapy in vivo with positron emission tomography. Cancer Res., 63: 3791–3798, 2003. Cancer Res. 2003;63:8558–9; author reply 8560.

Coombes JL, Robey EA. Dynamic imaging of host-pathogen interactions in vivo. Nat Rev Immunol. 2010;10:353–64.

Coombes JL, Charsar BA, Han SJ, Halkias J, Chan SW, Koshy AA, Striepen B, Robey EA. Motile invaded neutrophils in the small intestine of Toxoplasma gondii-infected mice reveal a potential mechanism for parasite spread. Proc Natl Acad Sci U S A. 2013;110:E1913–22.

Corstens FH, van der Meer JW. Nuclear medicine's role in infection and inflammation. Lancet. 1999;354: 765–70.

Culverwell AD, Scarsbrook AF, Chowdhury FU. False-positive uptake on 2-[(1)(8)F]-fluoro-2-deoxy-D-glucose (FDG) positron-emission tomography/computed tomography (PET/CT) in oncological imaging. Clin Radiol. 2011;66:366–82.

Davis SL, Nuermberger EL, Um PK, Vidal C, Jedynak B, Pomper MG, Bishai WR, Jain SK. Noninvasive pulmonary [18F]-2-fluoro-deoxy-D-glucose positron emission tomography correlates with bactericidal activity of tuberculosis drug treatment. Antimicrob Agents Chemother. 2009;53:4879–84.

del Rosal T, Goycochea WA, Mendez-Echevarria A, Garcia-Fernandez de Villalta M, Baquero-Artigao F, Coronado M, Marin MD, Albajara L. (1)(8)F-FDG PET/CT in the diagnosis of occult bacterial infections in children. Eur J Pediatr. 2013;172:1111–5.

Di Genaro MS, Waidmann M, Kramer U, Hitziger N, Bohn E, Autenrieth IB. Attenuated Yersinia enterocolitica mutant strains exhibit differential virulence in cytokine-deficient mice: implications for the development of novel live carrier vaccines. Infect Immun. 2003;71:1804–12.

Dorward DA, Lucas CD, Rossi AG, Haslett C, Dhaliwal K. Imaging inflammation: molecular strategies to visualize key components of the inflammatory cascade, from initiation to resolution. Pharmacol Ther. 2012;135:182–99.

Dumarey N, Egrise D, Blocklet D, Stallenberg B, Remmelink M, del Marmol V, Van Simaeys G, Jacobs F, Goldman S. Imaging infection with 18F-FDG-labeled leukocyte PET/CT: initial experience in 21 patients. J Nucl Med. 2006;47:625–32.

Eckert J, Deplazes P. Biological, epidemiological, and clinical aspects of echinococcosis, a zoonosis of increasing concern. Clin Microbiol Rev. 2004;17:107–35.

Freifeld AG, Bow EJ, Sepkowitz KA, Boeckh MJ, Ito JI, Mullen CA, Raad II, Rolston KV, Young JA, Wingard JR, et al. Clinical practice guideline for the use of antimicrobial agents in neutropenic patients with cancer: 2010 update by the infectious diseases society of america. Clin Infect Dis. 2011;52:e56–93.

Fuchs K, Kohlhofer U, Quintanilla-Martinez L, Lamparter D, Kotter I, Reischl G, Rocken M, Pichler BJ, Kneilling M. In vivo imaging of cell proliferation enables the detection of the extent of experimental rheumatoid arthritis by 3′-deoxy-3′-18f-fluorothymidine and small-animal PET. J Nucl Med. 2013a;54:151–8.

Fuchs K, Kukuk D, Mahling M, Quintanilla-Martinez L, Reischl G, Reutershan J, Lang F, Rocken M, Pichler BJ, Kneilling M. Impact of anesthetics on 3′-[18F] fluoro-3′-deoxythymidine ([18F]FLT) uptake in animal models of cancer and inflammation. Mol Imaging. 2013b;12:277–87.

Glaudemans AW, Signore A. FDG-PET/CT in infections: the imaging method of choice? Eur J Nucl Med Mol Imaging. 2010;37:1986–91.

Glaudemans AW, Quintero AM, Signore A. PET/MRI in infectious and inflammatory diseases: will it be a useful improvement? Eur J Nucl Med Mol Imaging. 2012;39:745–9.

Goldsmith SJ, Vallabhajosula S. Clinically proven radiopharmaceuticals for infection imaging: mechanisms and applications. Semin Nucl Med. 2009;39:2–10.

Griessinger CM, Kehlbach R, Bukala D, Wiehr S, Bantleon R, Cay F, Schmid A, Braumuller H, Fehrenbacher B, Schaller M, et al. In vivo tracking of Th1 cells by PET reveals quantitative and temporal distribution and specific homing in lymphatic tissue. J Nucl Med. 2014;55:301–7.

Haas H, Petrik M, Decristoforo C. An iron-mimicking, Trojan horse-entering fungi--has the time come for molecular imaging of fungal infections? PLoS Pathog. 2015;11:e1004568.

Hara T. 11C-choline and 2-deoxy-2-[18F]fluoro-D-glucose in tumor imaging with positron emission tomography. Mol Imaging Biol. 2002;4:267–73.

Hasenbach K, Wiehr S, Herrmann C, Mannheim J, Cay F, von Kurthy G, Bolmont T, Grathwohl SA, Weller M, Lengerke C, et al. Monitoring the glioma tropism of bone marrow-derived progenitor cells by 2-photon laser scanning microscopy and positron emission tomography. Neuro Oncol. 2012;14:471–81.

Holden VI, Bachman MA. Diverging roles of bacterial siderophores during infection. Metallomics. 2015;7:986–95.

Hot A, Maunoury C, Poiree S, Lanternier F, Viard JP, Loulergue P, Coignard H, Bougnoux ME, Suarez F, Rubio MT, et al. Diagnostic contribution of positron emission tomography with [18F]fluorodeoxyglucose for invasive fungal infections. Clin Microbiol Infect. 2011;17:409–17.

Jain SK, Kwon P, Moss WJ. Management and outcomes of intracranial tuberculomas developing during antituberculous therapy: case report and review. Clin Pediatr (Phila). 2005;44:443–50.

Jamar F, Buscombe J, Chiti A, Christian PE, Delbeke D, Donohoe KJ, Israel O, Martin-Comin J, Signore A. EANM/SNMMI guideline for 18F-FDG use in inflammation and infection. J Nucl Med. 2013;54:647–58.

Kircher MF, Gambhir SS, Grimm J. Noninvasive cell-tracking methods. Nat Rev Clin Oncol. 2011;8:677–88.

Knapp J, Bart JM, Giraudoux P, Glowatzki ML, Breyer I, Raoul F, Deplazes P, Duscher G, Martinek K, Dubinsky P, et al. Genetic diversity of the cestode Echinococcus multilocularis in red foxes at a continental scale in Europe. PLoS Negl Trop Dis. 2009;3:e452.

Langer O, Brunner M, Zeitlinger M, Ziegler S, Muller U, Dobrozemsky G, Lackner E, Joukhadar C, Mitterhauser M, Wadsak W, et al. In vitro and in vivo evaluation of [18F]ciprofloxacin for the imaging of bacterial infections with PET. Eur J Nucl Med Mol Imaging. 2005;32:143–50.

Lukawska JJ, Livieratos L, Sawyer BM, Lee T, O'Doherty M, Blower PJ, Kofi M, Ballinger JR, Corrigan CJ, Gnanasegaran G, et al. Real-time differential tracking of human neutrophil and eosinophil migration in vivo. J Allergy Clin Immunol. 2014;133(233–239):e231.

Maier FC, Kneilling M, Reischl G, Cay F, Bukala D, Schmid A, Judenhofer MS, Rocken M, Machulla HJ, Pichler BJ. Significant impact of different oxygen breathing conditions on noninvasive in vivo tumor-hypoxia imaging using [(1)(8)F]-fluoro-azomycinarabino-furanoside ([(1)(8)F]FAZA). Radiat Oncol. 2011;6:165.

Marik J, Junutula JR. Emerging role of immunoPET in receptor targeted cancer therapy. Curr Drug Deliv. 2011;8:70–8.

McKinley ET, Ayers GD, Smith RA, Saleh SA, Zhao P, Washington MK, Coffey RJ, Manning HC. Limits of [18F]-FLT PET as a biomarker of proliferation in oncology. PLoS One. 2013;8:e58938.

McKinley ET, Zhao P, Coffey RJ, Washington MK, Manning HC. 3′-Deoxy-3′-[18F]-Fluorothymidine PET imaging reflects PI3K-mTOR-mediated pro-survival response to targeted therapy in colorectal cancer. PLoS One. 2014;9:e108193.

Mejri N, Hemphill A, Gottstein B. Triggering and modulation of the host-parasite interplay by Echinococcus multilocularis: a review. Parasitology. 2010;137:557–68.

Mills B, Awais RO, Luckett J, Turton D, Williams P, Perkins AC, Hill PJ. [(18)F]FDG-6-P as a novel in vivo tool for imaging staphylococcal infections. EJNMMI Res. 2015;5:13.

Nakamura T, Takahashi O, Matsui K, Shimizu S, Setoyama M, Nakagawa M, Fukui T, Morimoto T. Clinical

prediction rules for bacteremia and in-hospital death based on clinical data at the time of blood withdrawal for culture: an evaluation of their development and use. J Eval Clin Pract. 2006;12:692–703.

Ning X, Seo W, Lee S, Takemiya K, Rafi M, Feng X, Weiss D, Wang X, Williams L, Camp VM, et al. PET imaging of bacterial infections with fluorine-18-labeled maltohexaose. Angew Chem Int Ed Engl. 2014;53:14096–101.

Nottebrock H, Then R. Thymidine concentrations in serum and urine of different animal species and man. Biochem Pharmacol. 1977;26:2175–9.

Parisi MT. Functional imaging of infection: conventional nuclear medicine agents and the expanding role of 18-F-FDG PET. Pediatr Radiol. 2011;41:803–10.

Petrik M, Haas H, Dobrozemsky G, Lass-Florl C, Helbok A, Blatzer M, Dietrich H, Decristoforo C. 68Ga-siderophores for PET imaging of invasive pulmonary aspergillosis: proof of principle. J Nucl Med. 2010;51:639–45.

Petruzzi N, Shanthly N, Thakur M. Recent trends in soft-tissue infection imaging. Semin Nucl Med. 2009;39:115–23.

Reuter S, Schirrmeister H, Kratzer W, Dreweck C, Reske SN, Kern P. Pericystic metabolic activity in alveolar echinococcosis: assessment and follow-up by positron emission tomography. Clin Infect Dis. 1999;29:1157–63.

Reuter S, Gruner B, Buck AK, Blumstein N, Kern P, Reske SN. Long-term follow-up of metabolic activity in human alveolar echinococcosis using FDG-PET. Nuklearmedizin. 2008;47:147–52.

Rolle AM, Soboslay PT, Reischl G, Hoffmann WH, Pichler BJ, Wiehr S. Evaluation of the metabolic activity of echinococcus multilocularis in rodents using positron emission tomography tracers. Mol Imaging Biol. 2015;17:512–20.

Rolle AM, Hasenberg M, Thornton CR, Solouk-Saran D, Mann L, Weski J, Maurer A, Fischer E, Spycher PR, Schibli R, et al. ImmunoPET/MR imaging allows specific detection of Aspergillus fumigatus lung infection in vivo. Proc Natl Acad Sci U S A. 2016;113(8):E1026–33.

Rosenbaum SJ, Lind T, Antoch G, Bockisch A. False-positive FDG PET uptake – the role of PET/CT. Eur Radiol. 2006;16:1054–65.

Santangelo PJ, Rogers KA, Zurla C, Blanchard EL, Gumber S, Strait K, Connor-Stroud F, Schuster DM, Amancha PK, Hong JJ, et al. Whole-body immunoPET reveals active SIV dynamics in viremic and antiretroviral therapy-treated macaques. Nat Methods. 2015;12:427–32.

Sarda L, Cremieux AC, Lebellec Y, Meulemans A, Lebtahi R, Hayem G, Genin R, Delahaye N, Huten D, Le Guludec D. Inability of 99mTc-ciprofloxacin scintigraphy to discriminate between septic and sterile osteoarticular diseases. J Nucl Med. 2003;44:920–6.

Schindler MK, Schutz MS, Muhlenkamp MC, Rooijakkers SH, Hallstrom T, Zipfel PF, Autenrieth IB. Yersinia enterocolitica YadA mediates complement evasion by recruitment and inactivation of C3 products. J Immunol. 2012;189:4900–8.

Shields AF, Grierson JR, Dohmen BM, Machulla HJ, Stayanoff JC, Lawhorn-Crews JM, Obradovich JE, Muzik O, Mangner TJ. Imaging proliferation in vivo with [F-18]FLT and positron emission tomography. Nat Med. 1998;4:1334–6.

Signore A, Glaudemans AW. The molecular imaging approach to image infections and inflammation by nuclear medicine techniques. Ann Nucl Med. 2011;25:681–700.

Signore A, Mather SJ, Piaggio G, Malviya G, Dierckx RA. Molecular imaging of inflammation/infection: nuclear medicine and optical imaging agents and methods. Chem Rev. 2010;110:3112–45.

Smith BA, Harmatys KM, Xiao S, Cole EL, Plaunt AJ, Wolter W, Suckow MA, Smith BD. Enhanced cell death imaging using multivalent zinc(II)-bis(dipicolylamine) fluorescent probes. Mol Pharm. 2013;10:3296–303.

Sorger D, Patt M, Kumar P, Wiebe LI, Barthel H, Seese A, Dannenberg C, Tannapfel A, Kluge R, Sabri O. [18F] Fluoroazomycinarabinofuranoside (18FAZA) and [18F]Fluoromisonidazole (18FMISO): a comparative study of their selective uptake in hypoxic cells and PET imaging in experimental rat tumors. Nucl Med Biol. 2003;30:317–26.

Stevens V, Geiger K, Concannon C, Nelson RE, Brown J, Dumyati G. Inpatient costs, mortality and 30-day re-admission in patients with central-line-associated bloodstream infections. Clin Microbiol Infect. 2014;20:O318–24.

Stumpe KD, Dazzi H, Schaffner A, von Schulthess GK. Infection imaging using whole-body FDG-PET. Eur J Nucl Med. 2000;27:822–32.

Tappe D, Kern P, Frosch M. A hundred years of controversy about the taxonomic status of Echinococcus species. Acta Trop. 2010;115:167–74.

Thornton CR, Wills OE. Immunodetection of fungal and oomycete pathogens: established and emerging threats to human health, animal welfare and global food security. Crit Rev Microbiol. 2015;41:27–51.

Tuzun M, Altinors N, Arda IS, Hekimoglu B. Cerebral hydatid disease CT and MR findings. Clin Imaging. 2002;26:353–7.

van Oosten M, Schafer T, Gazendam JA, Ohlsen K, Tsompanidou E, de Goffau MC, Harmsen HJ, Crane LM, Lim E, Francis KP, et al. Real-time in vivo imaging of invasive- and biomaterial-associated bacterial infections using fluorescently labelled vancomycin. Nat Commun. 2013;4:2584.

van Waarde A, Cobben DC, Suurmeijer AJ, Maas B, Vaalburg W, de Vries EF, Jager PL, Hoekstra HJ, Elsinga PH. Selectivity of 18F-FLT and 18F-FDG for differentiating tumor from inflammation in a rodent model. J Nucl Med. 2004;45:695–700.

Vinjamuri S, Hall AV, Solanki KK, Bomanji J, Siraj Q, O'Shaughnessy E, Das SS, Britton KE. Comparison of 99mTc infection imaging with radiolabelled white-cell imaging in the evaluation of bacterial infection. Lancet. 1996;347:233–5.

Vuitton DA, Gottstein B. Echinococcus multilocularis and its intermediate host: a model of parasite-host interplay. J Biomed Biotechnol. 2010;2010:923193.

Wang J, Yao WH, Yi BN, Liu S, Zhang DQ, Jiang CH, Zhang LM, Niu JQ, Jia WX, Wen H. Proton magnetic resonance spectroscopy in the evaluation of infiltration zone of cerebral alveolar echinococcosis. Chin Med J (Engl). 2012;125:2260–4.

Wang Y, Chen L, Liu X, Cheng D, Liu G, Liu Y, Dou S, Hnatowich DJ, Rusckowski M. Detection of Aspergillus fumigatus pulmonary fungal infections in mice with (99m)Tc-labeled MORF oligomers targeting ribosomal RNA. Nucl Med Biol. 2013;40:89–96.

Weinstein EA, Ordonez AA, DeMarco VP, Murawski AM, Pokkali S, MacDonald EM, Klunk M, Mease RC, Pomper MG, Jain SK. Imaging Enterobacteriaceae infection in vivo with 18F-fluorodeoxysorbitol positron emission tomography. Sci Transl Med. 2014;6:259ra146.

Wiehr S, Buhler P, Gierschner D, Wolf P, Rolle AM, Kesenheimer C, Pichler BJ, Elsasser-Beile U. Pharmacokinetics and PET imaging properties of two recombinant anti-PSMA antibody fragments in comparison to their parental antibody. Prostate. 2014;74:743–55.

WHO. World Health Statistics 2014; 2014.